Pergamon

Journal of Structural Geology, Vol. 20, No. 2/3, pp. 269 to 275, 1998

0191-8141/98 $19.00 + 0.00

PII: S0191-8141(97)00072-2

Fractal analysis of experimentally, dynamically recrystallized quartz grains and its possible application as a strain rate meter

MIKI TAKAHASHI*

Technical Research Center, Japan National Oil Corporation, 1-2-2 Hamada, Mihamaku, Chiba 261, Japan. e-mail: takhsi-m@jnoc.go.jp

HIROYUKI NAGAHAMA†

Institute of Geology and Paleontology, Tohoku University, Aoba, Aramaki, Aoba-ku, Sendai 980, Japan

TOSHIAKI MASUDA

Institute of Geosciences, Shizuoka University, 836 Oya, Shizuoka 422, Japan

and

AKIO FUJIMURA

Institute of Space and Astronautical Science, 3-1-1 Yoshinodai, Sagamihara, Kanagawa 229, Japan

(*Received* 20 *December* 1996; *accepted in revised form* 9 *September* 1997)

Abstract—Fractal analysis of experimentally recrystallized quartz grain shapes has been employed to study the relationship between the microstructures of dynamically recrystallized quartz grains and the deformation conditions such as temperature and strain rate. Samples used are quartz aggregates deformed under high temperature (800°C, 900°C and 1000°C) and high confining pressure (400 MPa). The fractal dimension is useful to quantify the shapes of the recrystallized quartz grain boundaries. At each set of conditions, the fractal dimension is determined as the slope of a log–log plot of the length of the grain boundaries (perimeters) against the grain size, calculated as diameters of circles having the same areas as the actual grains. The results show that the shapes of grains are self-similar, and the fractal dimensions, D, change systematically, being dependent on both temperature and strain rate. The skew of the grain boundary, defined as $D-1$, and showing the degree of the serration, may be proportional to the logarithm of the Zener–Hollomon parameter that includes a component of the Arrhenius term. This relation indicates that strain rate can be calculated from the fractal dimension and the temperature. It may therefore provide a new paleo-strain rate meter for plastically deformed natural rocks. © 1998 Published by Elsevier Science Ltd.

INTRODUCTION

Experimental studies of the syntectonic recrystallization of polycrystalline quartz have been carried out to simulate the development of natural microstructures in metamorphosed quartzite and to understand their formation conditions (e.g. Tullis *et al.*, 1973; Hara *et al.*, 1976; Masuda and Fujimura, 1981; Masuda, 1982; Karato and Masuda, 1989; Hirth and Tullis, 1992; Gleason *et al.*, 1993). The analysis of recrystallized microstructures of deformed quartz rocks might provide a key to deduce the physical conditions such as temperature and strain rate. Observing the photographs of thin sections from samples that were deformed under high temperature and high pressure (Fig. 1a), we can define a systematic shape change of the grain boundaries in conjunction with the deformation conditions. The grain boundaries become more serrated as the temperature is decreased and the strain rate is increased. They become more polygonal and linear as the temperature is increased and the strain rate is decreased. Masuda and Fujimura (1981) defined two types of grain boundaries: S-type for the serrated shape and P-type for the polygonal shape. If the transition between the grain boundary types is gradual, we can establish a microstructural parameter indicating the deformation conditions. The degree of serration of the grain boundaries would be connected with the deformation conditions (Jaoul *et al.*, 1984; Louis *et al.*, 1986). Thus, the shape of a grain boundary might be a useful microstructural parameter.

In the study of hot-worked metal, fractal analysis was applied to quantify the shape of grain boundaries (Hornborgen, 1987; Tanaka and Iizuka, 1991). Hornborgen (1987) found an increase of fractal dimension with strain, in hot-worked tests of CuZnAl solid solution. Tanaka and Iizuka (1991) investigated the fractal grain boundary of hot-resistant alloys and found a relation

* Corresponding author.
† Present address: Institute of Geophysics, Polish Academy of Sciences, ul. Księcia Janusza 64, 01-452, Warszawa 64, Poland.

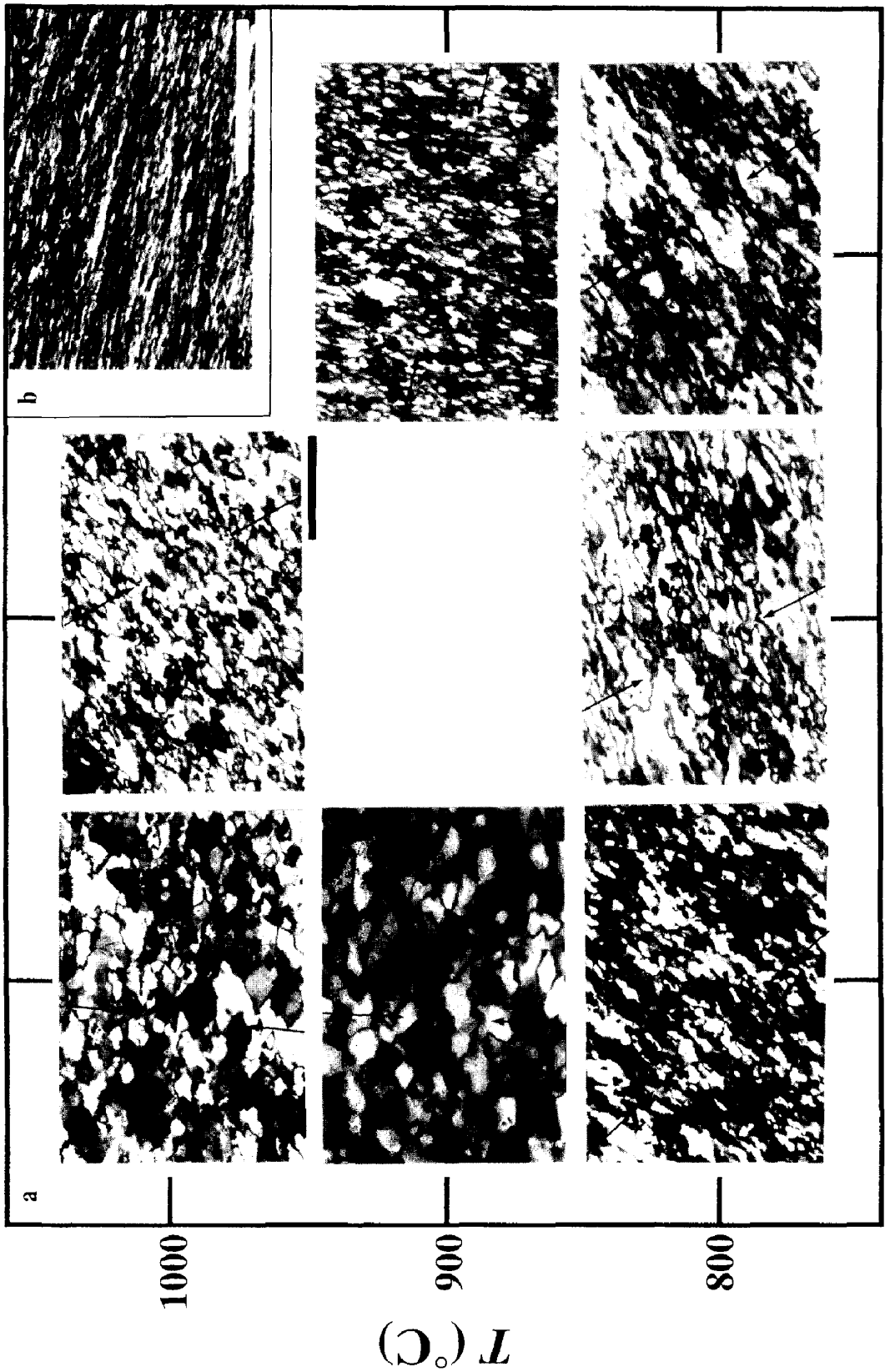

Fig. 1. (a) The seven photographs relating to experimental temperature and strain rate, showing microstructures of the central parts of the experimental specimens. See also Table 1. Scale bar is 200 μm. Arrows indicate the direction of compression. Three samples are from Masuda and Fujimura (1981), and four new samples are from the same Griggs type apparatus. The deformation conditions were: 400 MPa confining pressure, 800°C, 900°C, 1000°C and 10^{-4}, 10^{-5} and 10^{-6} (s^{-1}) strain rates. The starting materials were agate. (b) Photomicrograph of the starting material, Minas agate, used in the new experiments. Scale bar is 1 mm.

that the ratio of rupture ductility increased with the fractal dimension difference between serrated and straight grain boundary specimens. Recently, the fractal dimension of quartz grain boundaries has been suggested by Kruhl and Nega (1996) as a geothermometer. They investigated the fractal dimensions of quartz grain boundaries in different grades of metamorphic and igneous rocks, and found that the dimensions decrease with increasing temperature. The fractal dimension of grain shapes is considered to be statistically one of the measures of microstructure. When the fractal dimension of grain shapes is almost one, the grain boundaries display linear shapes, and when the fractal dimension shows a higher value, towards 2, the grain boundaries present a serrated figure.

Because there is an extrapolation rule between temperature and time (so-called 'temperature-compensated time') in rheological studies (Shimamoto, 1987; Nagahama, 1994), it is consequently natural to investigate the skew of the grain boundaries (departure from polygonal shapes) changing with the strain rate. Here, our objective is an investigation of the relation between grain shapes and deformation conditions, using fractal analysis for the quantification of the grain boundary shapes. We conclude that fractal analysis of quartz rocks is a good indicator not only of temperature, but also of strain rate. In our study, we make use of three experimentally deformed samples for the analysis. Those experiments were done by Masuda and Fujimura (1981). We also make use of four previously unpublished experimental samples that were obtained using the same apparatus. The experimental conditions and the deformed microstructures of those seven samples are shown in Table 1 and Fig. 1.

EXPERIMENTAL PROCEDURE

A detailed account of the experimental apparatus is given in Masuda and Fujimura (1981). Only the important information is given below.

A triaxial, constant-strain-rate apparatus was used for these high temperature–pressure experiments. Cylindrical specimens 10 mm in diameter and $8 \sim 18$ mm in length were compressed uniaxially by a pair of inner pistons. One of these pistons was driven by an electric motor through a ball-screw actuator and a gear train. Axial compression by a pair of outer pistons through a hydraulic ram produced a confining pressure that was transmitted to the specimen through a pyrophyllite medium. The specimen was heated by a graphite tube heater surrounded by the pyrophyllite medium, and the specimen was sheathed with a thin pyrophyllite sleeve in order not to touch the graphite tube heater directly. The temperature of the specimen was measured by a NiAl–CrAl thermocouple at the center of the surface of the specimen. The temperature gradient in each specimen was less than $10°C\,mm^{-1}$. For analyzing the microstructures, we chose the central area ($240 \times 350\ \mu m^2$) of thin sections cut parallel to the axial loading and passing through the center of the cylindrical specimens.

The axial force was not measured on the Minas agate specimens (unpublished data) but only on the Okutodami agate specimens described in Masuda and Fujimura (1981). Measurement of the axial force was made by a load cell attached to the inner piston for axial deformation. Because of the friction between the pressure medium and the pistons, there may be a difference of up to ± 150 MPa between the true stress and that calculated from the reading of the axial force by the load cell. From the stress–strain curves of Masuda and Fujimura (1981), the differential stress does not reach a steady state. As a result, we cannot discuss the power law relation between steady-state stress and average grain size due to inaccuracy and lack of measurement of axial forces.

The experimental conditions are summarized in Table 1. All runs were conducted at 400 MPa confining pressure, at temperatures of $800 \sim 1000°C$, and with a strain rate in the range $10^{-4} \sim 10^{-6}\ s^{-1}$. The confining pressure and temperature lie in the stability field of β-quartz. Because temperature falls below 100°C within a few minutes after the end of runs, we can dismiss any recovery of grain boundary migration by post-deformation annealing. The deformation was produced under wet conditions, because pyrophyllite releases H_2O above approximately 520°C at 400 MPa of confining pressure, and the specimens themselves include H_2O. However, we did not quantify the water in the sample assembly. The Masuda and Fujimura (1981) experiments used Okutadami agate (Japan), whereas the others used Minas agate

Table 1. Experimental conditions and results of microstructural analysis

T (°C)	log [$\dot{\varepsilon}$ (s^{-1})]	Confining pressure (MPa)	ε (%)	D	N	r	Starting material
1000	−6	400	10	1.03±0.07	94	0.97	Okutadami agate*
1000	−5	400	20	1.16±0.07	62	0.97	Okutadami agate*
800	−6	400	44	1.14±0.06	142	0.97	Okutadami agate*
800	−4	400	31	1.30±0.07	77	0.97	Minas agate
800	−5	400	40	1.22±0.07	75	0.96	Minas agate
900	−4	400	30	1.26±0.07	77	0.97	Minas agate
900	−6	400	11	1.05±0.07	68	0.96	Minas agate

The confining pressure was solid pressure. Samples used are from Masuda and Fujimura (1981) (*), and previously unpublished data.
N is the number of quartz grains used in this fractal analysis, and D is the fractal dimension.

(Brazil). The optical structure of both starting materials was very similar, and any difference between the two was assumed to disappear through recrystallization during the pre-experimental heating, and grain growth.

In our evaluation of the experimental procedure, the fractal analyses provide useful information for the relation of the shapes of recrystallized quartz grain boundaries and the deformation conditions. However, we need to develop an experimental methodology (e.g. quantifying water in specimens of pyrophyllite or measuring the differential stress) for further quantification of this relationship.

THE METHOD OF FRACTAL ANALYSIS

The method for determining a fractal dimension, D, is explained below. Because of the temperature gradient in specimens, we used only the center part of the specimens for the analysis. First, more than 50 grains, which displayed the grain boundaries clearly, were chosen. The boundaries were traced from a nearly central area ($240 \times 350\ \mu m^2$) of the specimen from photographs of thin sections. To avoid tracing subgrain boundaries, we identified each grain boundary by revolving the stage of the optical microscope. The actual perimeters, P, and areas, A, of these traced grains were determined by imaging software measuring the number of pixels ($10\ \mu m = 160 \pm 5$ pixels). The areas were measured to calculate the diameters, d, of circles having the same areas. By log–log plotting the actual perimeters, P, on the vertical axis and the grain sizes, d, on the horizontal axis, the fractal dimension, D, is defined as the slope of a least-squares fitted line for each set of deformation conditions. The method is the same as for the area–perimeter relation for rain and cloud published by Mandelbrot (1977) and Lovejoy (1982). Thus, we can compare a perimeter length of the grain boundary, P, and a length of the circumference having the same area as a grain, πd. This schematic explanation is illustrated in Fig. 2, and the expected relation is:

$$P \propto d^D. \tag{1}$$

Thus, the fractal dimensions are calculated by comparison of the grain diameters and the perimeters. Because the analysis is two-dimensional, using a thin section photograph, the range of the fractal dimension is $1 \leq D \leq 2$.

RESULTS

Using the perimeter–diameter relation, a fractal dimension of grain shapes is obtained by the slope of a plot of log P vs log d. The results are shown in Fig. 3. The correlation coefficients show a value of more than 0.96, and the errors of fractal dimensions show a standard

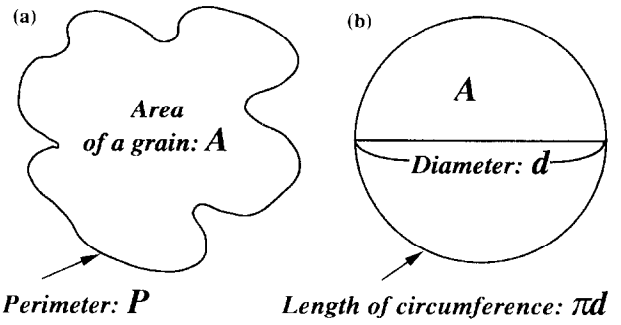

Fig. 2. The concept of the fractal analysis shown schematically. (a) A quartz grain having the area, A, and serrated perimeter, P. (b) Circle has the same area, A, and diameter, d. The actual length of the grain boundary, P, is longer than the circumference of the corresponding circle. The circumference of the circle is proportional to the diameter, but this may not be true for the serrated boundary. Thus, one may characterize the complexity of serrated grain boundaries by comparing the perimeters with the diameter.

error of less than ± 0.07. The shapes of the grain boundaries for the measured sizes are self-similar statistically. The dimensions increase with strain rate, $\dot{\varepsilon}$ (Fig. 3a) and decrease with temperature, T (Fig. 3b), so the fractal dimension changes systematically with changing conditions. The fractal dimension therefore would be an indicator of a set of deformation conditions.

If we can regard the fractal dimension as a parameter of the deformation conditions, then the relation between the fractal dimension, D, temperature, T (in K), and strain rate, $\dot{\varepsilon}$ (s^{-1}), is obtained by least-square linear fitting:

$$D = \phi \log \dot{\varepsilon} + \frac{\rho}{T} + 1.08, \tag{2}$$

where $\phi = 9.34 \times 10^{-2}$ $\{[\log(s^{-1})]^{-1}\}$ and $\rho = 6.44 \times 10^2$ (K). From this equation, contours of the fractal dimensions can be drawn on a graph where axes are the deformation conditions, $1/T$ and $\dot{\varepsilon}$ (Fig. 4). Comparing each interval of the contour lines, errors of fractal dimensions analyzed on seven experiments (less than ± 0.07) are larger than the intervals necessary to discuss the reliability of this equation. However, the increasing tendency of fractal dimension is clearly related to increasing values of the deformation conditions, $1/T$ and $\dot{\varepsilon}$.

Because we measured the fractal dimension in a plane, the fractal dimension minus 1, $D-1$, indicates the degree of serration of the grain boundary and is defined as the skew of the grain boundary. Equation (2) indicates that the skew of grain boundary, $D-1$, is approximately proportional to the Arrhenius terms, $\ln \dot{\varepsilon} + Q/RT$:

$$D - 1 \approx \Phi\left(\ln \dot{\varepsilon} + \frac{Q}{RT}\right), \tag{3}$$

where Q is the activation energy for flow involving dynamic recrystallization at high temperature, R is the universal gas constant, and $\Phi = 0.04$ $\{[\ln(s^{-1})]^{-1}\}$. From equation (2) and this Arrhenius term [equation (3)], we

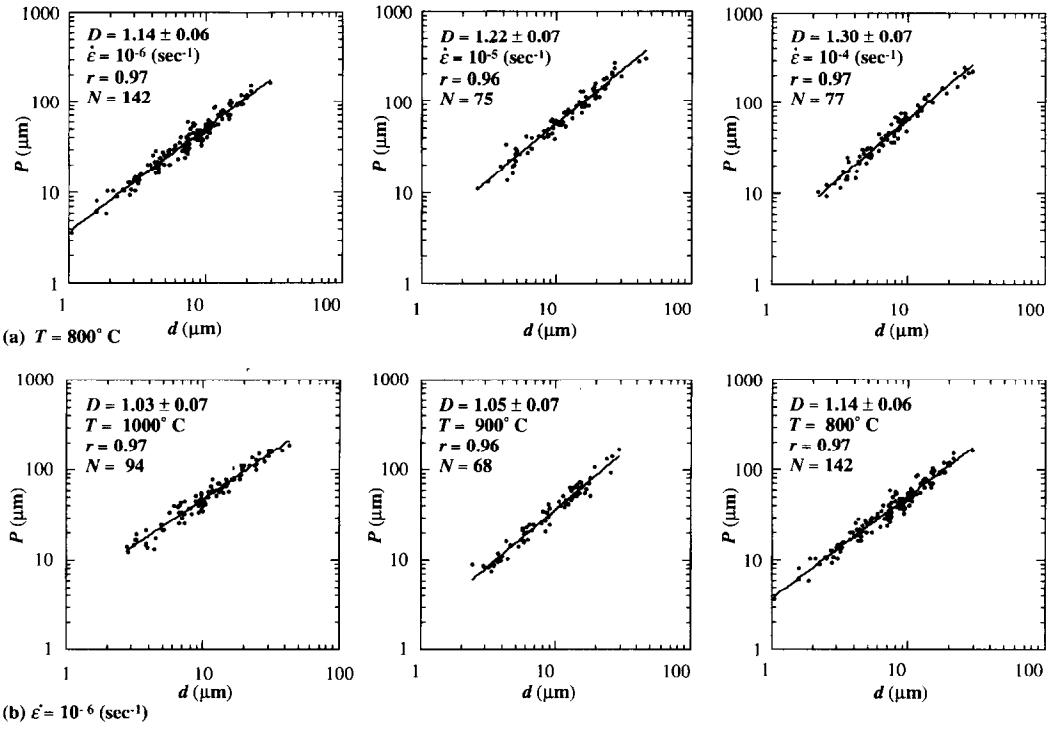

Fig. 3. Measured perimeters, P, of the grain boundaries plotted against grain size, d. Least-square linear fits of the perimeters against the diameters on the log–log plot are shown, and the fractal dimensions are given by the slopes of the lines. r is the correlation coefficient, and N is the number of grains used in the analysis. The error is determined as the standard deviation. (a) Comparison of the fractal dimensions with the strain rates increasing at a constant temperature, 800°C. (b) Comparison of the fractal dimensions with the temperatures decreasing at a constant strain rate, 10^{-6} (s^{-1}).

can calculate the activation energy of the deformation and/or recrystallization of quartz aggregates in this set of experiments; from which $Q = 132$ (errors are $+45$ and -36) kJ mol^{-1} ($Q = R\rho \ln 10 / \phi$). The errors are required from standard errors of ϕ and ρ. Although we cannot discuss the deformation mechanics from the value of the activation energy because structures of dislocations were not observed, this value of the activation energy of recrystallizing quartz agrees with some other experiments on wet quartzite deformed by dislocation creep (e.g. Koch *et al.*, 1989; Gleason and Tullis, 1995). Here, we made an assumption that the amounts of water are approximately similar for each sample that we used. From the results of Post *et al.* (1996), we also assume that the amount of water in the specimens can only affect the deformational stress and the fine detail of the dislocation creep regime in the specimens that we studied.

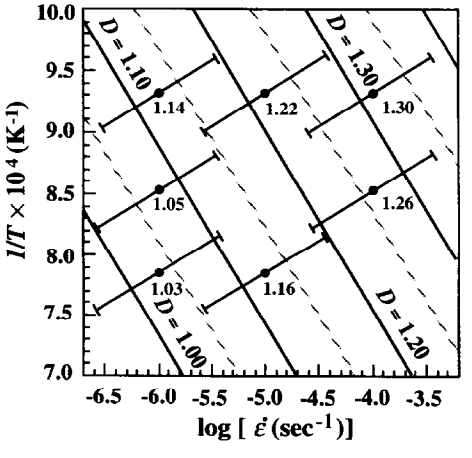

Fig. 4. The relation between fractal dimension and the deformation conditions. The values shown are the fractal dimensions at each experimental condition (marked by the spots). The contour lines are determined from equation (2), from the fractal dimensions of the seven results by multiple linear regression.

DISCUSSIONS

Applying the fractal concept to quartz grain boundaries, the fractal dimension may be a good indicator of strain rate and/or temperature, allowing the inference of one if the other is known. However, there are some problems to be discussed.

This fractal approach to understanding the dynamics of the recrystallized condition is based on the morphology of the grain boundaries, and does not involve the mechanism of recrystallization. Masuda and Fujimura (1981) also defined the P-type and S-type optical grain shapes morphologically. Using optical and TEM observations in experimentally deformed quartz aggregates, Hirth and Tullis (1992) and Gleason *et al.* (1993) determined three regimes of dislocation creep mechani-

cally. They are dependent on the relative rates of grain boundary migration, dislocation climb and dislocation production. At lower temperatures and higher strain rates (named regime 1), the strain-induced grain boundary migration accommodates the recovery resulting from too great a rate of dislocation production. With an increase in temperature and a decrease in strain rate (regime 2), dislocation climb causes recovery accommodated by progressive subgrain rotation. With even higher temperatures and lower strain rates (regime 3), dynamic recrystallization occurs by both dislocation climb and migration recrystallization. Comparing the optical microphotos of Fig. 1(a) with the results of Hirth and Tullis (1992), a transition from S-type to P-type would correspond to the transition from regime 2 and/or regime 3 to the regime where the rate of grain boundary migration becomes greater than that of dislocation climb. The core and mantle structures, which show regimes 2 and 3, are observed at a lower temperature (800°C) and higher strain rate (10^{-5} and 10^{-4} s^{-1}). Without TEM observation for our samples, we cannot distinguish exactly which mechanics correspond to regime 2 or 3 (indicating the core and mantle structures) of our samples. If this assumption is true, the estimated activation energy of dislocation creep, $Q = 132$ (errors are $+45$ and -36) kJ mol^{-1}, from equation (3) might correspond to that of dislocation climb and/or migration recrystallization. Experiments in which the amount of water in the specimens is controlled and the differential stress is measured will clarify this point in the future.

The empirical Dorn equation has long been used to describe the results of steady-state creep tests on materials at high temperature. It is a constitutive law given as

$$\dot{\varepsilon} \propto \sigma^n \exp(-Q/RT), \tag{4}$$

where σ is the differential stress and n is a constant defining the stress sensitivity of the strain rate. The differential stress depends on the Arrhenius terms and can be generalized as

$$F(\sigma) \propto \dot{\varepsilon} \exp(Q/RT) = Z, \tag{5}$$

where Z is generally called the Zener–Hollomon parameter (Poirier, 1985; Sakai, 1989). From equation (4), the Zener–Hollomon parameter is a function of the differential stress. The differential stress reflects the microstructure (Poirier, 1985) that we recognized as the grain shapes in this case. The Zener–Hollomon parameter also gives an extrapolation rule of temperature-compensated time between experimental conditions and nature (e.g. Shimamoto, 1987; Nagahama, 1994). Now, from equations (3) and (5), the relation between the fractal dimension and the Zener–Hollomon parameter can be described as

$$D - 1 \propto \ln Z. \tag{6}$$

As both terms, D and Z, can be defined by the structural parameter, the comparison between them is reasonable.

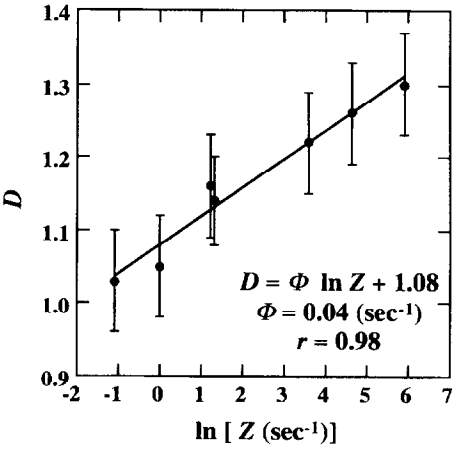

Fig. 5. The fractal dimension, D, plotted against the Zener–Hollomon Parameter, Z, on a semi-log plot. The activation energy estimated, Q, is 132 kJ mol^{-1}. r is the correlation coefficient.

It is also clear from Fig. 5 that the fractal dimension as a indication of grain boundary shape relates to the Arrhenius term or the Zener–Hollomon parameter. The Zener–Hollomon parameter at constant stress deformation depends on the stress sensitivity exponent n and on the fractal dimension of the grain shape (the skew of grain boundaries), as has already been pointed out by Nagahama (1994).

Gleason *et al.* (1993) deformed a series of flint samples with the progressive development of strain under constant conditions (900°C and 10^{-5} s^{-1} strain rate). With increasing strain (14 ~ 75%), the optical microstructures of deformed quartz [see Gleason *et al.* (1993), fig. 6] changed the grain boundary shapes from P-type to S-type. In that case, the fractal dimension would increase with strain. Hornborgen (1987) also observed that the fractal dimensions of brass alloy grain boundaries developed progressively with plastic deformation. In this study, however, we did not detect any change of the fractal dimensions with increasing strain. Further research on the development of the fractal dimension with strain must be carried out.

Last, we must discuss the extrapolation of this theory to nature. There are some difficulties with the application of the method, even apart from the accuracy of the experiments. Comparing nature with the laboratory, the deformation conditions such as temperature, pressure and strain rate are not constant during metamorphism, and grain boundary serration will tend to be deleted by post-deformation annealing. Most high-temperature and high-pressure deformation experiments on quartz aggregates have been made in the β-quartz stability field. However in nature, rock deformation usually occurs in the α-quartz stability field. If the activation energy for dislocation creep changes at the α–β transition, the slope of the fractal contour lines in Fig. 4 must change during natural metamorphic conditions. Additionally, as implied by Hirth and Tullis (1992), the activation energy might change between each regime of dislocation creep.

Because we have only seven experimental samples, more detailed verifications could not be made at present.

CONCLUSIONS

From the relationship between the perimeters and diameters of quartz grains, the shapes of experimentally deformed grains show statistical self-similarities at each set of deformation conditions. The fractal dimension systematically increases with increasing strain rate and decreasing temperature. We propose the fractal dimension as a new paleo-strain rate meter for plastically deformed rocks, provided that temperature is known from other data, such as metamorphic mineral assemblage. The relation between the fractal dimension and the Arrhenius terms is:

$$D = \phi \log \dot{\varepsilon} + \frac{\rho}{T} + 1.08$$

where $\phi = 9.34 \times 10^{-2}$ $\{[\log(s^{-1})]^{-1}\}$ and $\rho = 6.44 \times 10^{2}$ (K), and this is expected to apply over a range of stress levels. From the Arrhenius term, the activation energy is estimated at 132 (errors are $+45$ and -36) kJ mol^{-1}. This value is consistent with that obtained from wet quartz-rocks deformed experimentally in the dislocation creep field.

A proportionality was found between the skew of the grain boundary, $D-1$, and the natural log of the Zener–Hollomon parameter, ln Z. This would imply that the stress sensitivity of the strain rate depends on the skew of the grain boundaries.

Although there are presently some uncertainties in extrapolation of the method to nature, by measuring the fractal dimension of grain shapes of naturally recrystallized quartzite, and knowing metamorphic temperature by metamorphic minerals, we should be able to estimate the paleo-strain rate of the rocks provided that the microstructures of quartz have been preserved.

Acknowledgements—The authors thank K. Michibayashi and B. MacNeil for criticism of the manuscript, and S. Sugita and S. Suzuki for access to unpublished data. The authors also thank T. Shimamoto and J. H. Kruhl for the valuable comments. The thorough and helpful comments from E. H. Rutter, J. Tullis and an anonymous reviewer are gratefully acknowledged.

REFERENCES

Gleason, G. C., Tullis, J. and Heidelbach, F. (1993) The role of dynamic recrystallization in the development of experimentally deformed quartz aggregates. *Journal of Structural Geology* **15**, 1145–1168.

Gleason, G. C. and Tullis, J. (1995) A flow law for dislocation creep of quartz aggregates determined with the molten salt cell. *Tectonophysics* **247**, 1–23.

Hara, I., Paulitsch, P., Nishimura, Y. and Tanaka, K. (1976) Subbasal II Lamellae in naturally deformed quartz. *Neues Jahrbuch fur Mineralogie Abhandlungen* **126**, 254–268.

Hirth, G. and Tullis, J. (1992) Dislocation creep regimes in quartz aggregates. *Journal of Structural Geology* **14**, 145–159.

Hornborgen, E. (1987) Fractal analysis of grain boundaries in hot-worked poly-crystals. *Zeitschrift fur Metallkunde* **78**, 622–625.

Jaoul, O., Tullis, J. and Kronenberg, A. (1984) The effect of varying water contents on the creep behavior of Heavitree quartzite. *Journal of Geophysical Research* **89**, 4298–4312.

Karato, S.-I. and Masuda, T. (1989) Anisotropic grain growth in a quartz aggregate under stress and its implications for foliation development. *Geology* **17**, 695–698.

Koch, P. S., Christie, J. M., Ord, A. and George, R. P. Jr. (1989) Effect of water on the rheology of experimentally deformed quartzite. *Journal of Geophysical Research* **94**, 13975–13996.

Kruhl, J. H. and Nega, M. (1996) The fractal shape of sutured quartz grain boundaries: application as a geothermometer. *Geologishe Rundschau* **85**, 38–43.

Louis, E., Guinea, F. and Flore, F. (1986) The fractal nature of fracture. In *Fractals in Physics*, eds L. Pietronero and E. Tosatti, pp. 177–180. Elsevier, Amsterdam.

Lovejoy, S. (1982) Area–perimeter relation for rain and cloud areas. *Science* **216**, 185–187.

Mandelbrot, B. (1977) *Fractals*. W. H. Freeman, San Francisco.

Masuda, T. (1982) A microstructural sequence of quartz schists in central Shikoku, southwest Japan. *Tectonophysics* **83**, 329–345.

Masuda, T. and Fujimura, A. (1981) Microstructural development of fine-quartz aggregates by syntectonic recrystallization. *Tectonophysics* **72**, 105–128.

Nagahama, H. (1994) High-temperature viscoelastic behavior and long time tail of rocks. In *Fractal and Dynamical Systems in Geoscience*, ed. J. H. Kruhl, pp. 121–129. Springer-Verlag, Berlin.

Poirier, J.-P. (1985) *Creep of Crystals*. Cambridge University Press, Cambridge.

Post, A. D., Tullis, J. and Yund, R. A. (1996) Effect of chemical environment on dislocation creep of quartzite. *Journal of Geophysical Research* **101**, 22143–22155.

Sakai, T. (1989) Dynamic recrystallization of metallic materials. In *Rheology of Solids and of the Earth*, eds S. Karato and M. Toriumi, pp. 284–307. Oxford University Press, New York.

Shimamoto, T. (1987) High temperature viscoelastic behavior of rocks. *Proceedings of the 7th Japan Symposium on Rock Mechanics* 467–472 (in Japanese with English abstract).

Tanaka, M. and Iizuka, H. (1991) Characterization of grain boundaries by fractal geometry and creep-rupture properties of heat-resistant alloys. *Zeitschrift fur Metallkunde* **82**, 422–447.

Tullis, J., Christie, J. M. and Griggs, D. T. (1973) Microstructure and preferred orientations of experimentally deformed quartzites. *Geological Society of America Bulletin* **84**, 297–314.